A Model of Calcium Dynamics in Cardiac Myocytes Based on the Kinetics of Ryanodine-Sensitive Calcium Channels

Yuanhua Tang and Hans G. Othmer
Department of Mathematics, University of Utah, Salt Lake City, Utah 84112 USA

ABSTRACT The ryanodine-sensitive calcium channels are pivotal to signal transduction and cell function in many cell types, including cardiac myocytes. In this paper a kinetic model is proposed for these channels. In the model there are two Ca regulatory sites on the channel protein, one positive and the other negative. Cytoplasmic Ca binds to these regulatory sites independently. It is assumed that the binding of Ca to the positive site is a much faster process than binding to the negative site. At steady state, the channel opening as a function of the Ca concentration is a bell-shaped curve. The model predicts the adaptation of channels to constant Ca stimulus. When this model is applied to cardiac myocytes, it predicts excitability with respect to Ca perturbations, smoothly graded responses, and Ca oscillations in certain pathological circumstances. In a spatially distributed system, traveling Ca waves in individual myocytes exist under certain conditions. This model can also be applied to other systems where the ryanodine-sensitive channels have been identified.

INTRODUCTION

CALCIUM DYNAMICS IN CARDIAC MUSCLES

Muscle cells use calcium (Ca) as the specific second messenger for transducing an external signal into fiber contraction. The external signal is electrical depolarization of the sarcolemmal membrane in cardiac myocytes. The depolarization results in an increase in the cytoplasmic Ca, which then causes the muscle fibers to contract. This process is usually called excitation-contraction coupling, or simply E-C coupling (Bers, 1991). The depolarization of the sarcolemmal membrane triggers a Ca influx from the extracellular medium by opening voltage-sensitive Ca channels and reversing the conducting direction of the Na/Ca exchangers in the membrane. This initial Ca influx from the extracellular medium binds with receptors that are part of the ryanodine-sensitive Ca channels (RyR) embedded in the membrane of the sarcoplasmic reticulum (SR). Upon binding of Ca the channel opens, and Ca stored in the SR diffuses through the channel into the cytosol. This larger secondary Ca release into the cytoplasm, together with the initial Ca influx, causes a large increase in the cytosolic Ca concentration. The cytosolic Ca binds with troponin C to initiate muscle contraction.

Superthreshold electrical excitation of the surface membrane leads to an action potential that propagates as a wave of depolarization along the surface and along the transverse tubules on a very fast time scale. The membrane depolarization lasts about 250 ms (Katz, 1992), and a typical speed of the depolarization wave is 0.3–1.0 $m \cdot s^{-1}$ in ventricular myocardium and even faster in Purkinje fibers. Given a length of 100 μm for a typical myocardium, the electrical wave depolarizes the entire membrane within about ~0.1 ms. On the other hand, the increase of Ca in the cytosol is on the time scale of several hundred ms. Hence, the spread of the depolarization wave across the membrane can be considered instantaneous in the study of intracellular Ca dynamics under normal circumstances.

In this paper we will concentrate on modeling of the Ca dynamics in myocytes; the electrical aspects will be ignored. The membrane depolarization will simply be modeled by a stepwise Ca entry current. A schematic diagram of the components involved in the model is shown in Fig. 1. In the sarcolemma there are Ca channels that are responsible for Ca entry into the cytosol upon depolarization. The Ca-ATPase and Na/Ca exchanger are primarily responsible for pumping Ca out of the cytoplasm against the Ca electrochemical gradient across the membrane. In this model, the effect of Ca-ATPase and the Na/Ca exchanger is combined into a single Ca pump, since Na is not a component of the model. The primary intracellular Ca store is the SR. Ca enters the cytosol from the SR via RyR and is pumped back into the SR by a Ca pump located on the SR membrane. In addition, there is leakage of Ca both from the extracellular medium and from the SR into the cytosol. Although the scheme depicted in Fig. 1 is a drastic simplification of Ca regulation in myocytes, it will be shown that such a simple scheme can explain the essential phenomena observed in myocytes.

Regulation of the RyR on SR membrane

The essential component of Ca dynamics in the model is the kinetics of RyR in the SR membrane. The purified RyR exists as a tetramer of four identical subunits, resembling a four-leaf clover in appearance. It has four distinct conducting levels, and each level is probably regulated by a single subunit of the complex. Each subunit can conduct at the ~30 pS level

Received for publication 26 May 1994 and in final form 15 September 1994.
Address reprint requests to Dr. Yuanhua Tang at his current address, Department of Physiology and Biophysics, Cornell University Medical College, New York, NY 10021. Tel.: 212-746-6361; Fax: 212-746-8690; E-mail: tang@figaro.med.cornell.edu.

0006-3495/94/12/2223/13 $2.00

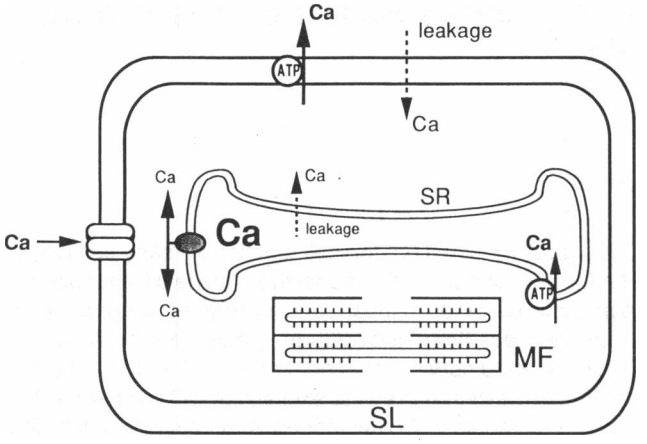

FIGURE 1 A schematic diagram of Ca regulation in cardiac myocytes, modified from Bers (1991). In the sarcolemma there are voltage-sensitive Ca channels, Ca-ATPase, and the Na/Ca exchanger. On the SR membrane there are the RyR and Ca pump. Ca can also enter the cytosol through leakage from the SR and the extracellular medium.

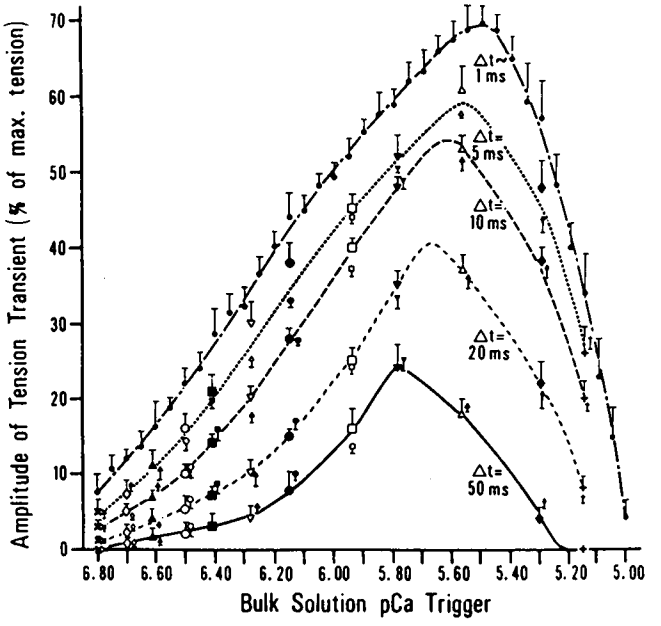

FIGURE 2 The relationship between the bulk solution pCa at the peak of free Ca used as a trigger, and the amplitude of the tension transient at various durations (Δt) taken for the increase of Ca in the solution bathing the skinned cell. From Fabiato (1985) with permission.

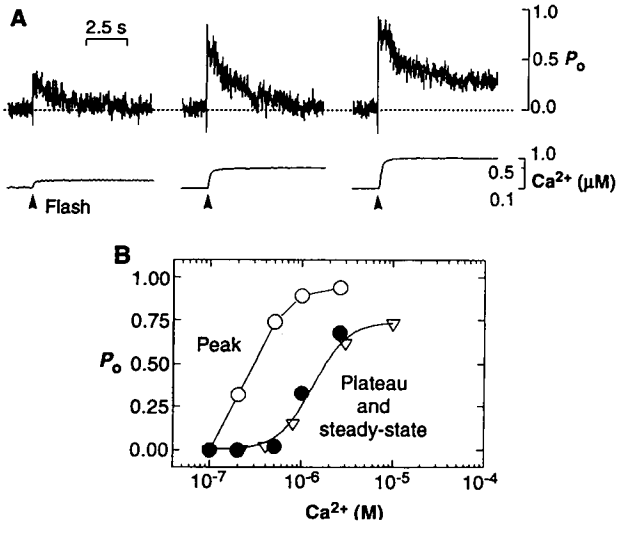

FIGURE 3 Adaptation experiments on channel opening in response to photolysis of caged Ca. (*A*) The averaged channel opening of 64 individual channels in response to Ca stimuli of 0.1 μM, 0.5 μM, and 1.0 μM. (*B*) Dependence of channel opening on [Ca] at the peak (○) and steady state response (●). From Györke and Fill (1993) with permission.

(Liu et al., 1989). The most probable conducting state is one of 100 ± 10 pS unitary Ca conductance, indicating that there is cooperativity among the regulation of the subunits (Liu et al., 1989; Lai et al., 1989; Saito et al., 1988).

Fabiato (1985) performed extensive studies on the characteristics of Ca-induced Ca release (CICR) in mechanically-skinned single cardiac myocytes. He demonstrated that Ca release is triggered by a rapid increase of Ca at the outer surface of the SR of a previously quiescent cell under physiological conditions. Increasing the stimulatory Ca trigger increased the Ca released up to a maximal level. A higher stimulatory Ca is called superoptimum, and such stimuli actually inhibit CICR. The relationship between the triggering Ca and the amplitude of tension transient of the muscle fiber induced by the released Ca is shown in Fig. 2. Partial inactivation of Ca release by stimulatory Ca is also observed for low-level stimuli. The opening of the channels depends not only on the concentration of stimulatory Ca but also on how it is applied. The faster a certain amount of Ca is applied, the tighter the muscle contracts (Fig. 2). The channel dynamics of activation and inactivation in response to Ca stimuli appears to be both time and Ca dependent. The same type of channel behavior has been confirmed by using either SR heavy vesicles or by using reconstituted channels in lipid bilayers. The measurements made at the individual channel level also point to such channel dynamics (Meissner et al., 1991; Györke and Fill, 1993).

The time-dependent aspect of channel dynamics stems from the fact that they adapt to Ca stimuli (Györke and Fill, 1993). Györke and Fill performed their experiments on RyR embedded in a lipid bilayer (see Fig. 3). The stimulus to the channels is obtained through photolysis of caged Ca. By averaging the channel dynamics of several dozen individual channels, they found that RyRs adapted to a maintained Ca stimulus while retaining their ability to respond to a second Ca stimulus. One interesting aspect of this adaptation is that it is not a complete adaptation, as in *Dictyostelium discoideum* (Tang and Othmer, 1994). As the concentration of Ca applied approaches the μM range, the unadapted fraction of open channels becomes quite significant (Fig. 3). This experiment is a confirmation of Fabiato's (1985) work on the skinned cardiac

myocytes discussed earlier. The unadapted portion in the paper by Györke et al. coincides with a point on the bell-shaped curve for the steady-state channel opening in Fabiato's paper. As one can see, the steady-state channel opening is quite substantial in the optimal range of stimuli (Fabiato, 1985).

A biochemical model for the channel dynamics proposed by Fabiato (1992) is shown in Fig. 4. In the model there are two regulatory Ca binding sites on the cytoplasmic side of the channel. One is positively regulatory and the other negatively regulatory. Ca binding to the positive site is fast but has a low affinity, whereas binding of Ca to the negative site is slower, but has a higher affinity. The channel can exist in four states: the bare receptor (activatable), the receptor with Ca in only the positive site (open), the receptor with Ca in both positive and negative sites (closed), and the receptor with Ca on the negative site only. The last state represents a refractory state in which the channel is not responsive to stimuli.

Fabiato's (1992) model was proposed before the work of Györke and Fill (1993), and it predicts channel adaptation in response to step changes in Ca. The initial response to a Ca stimulus is the binding of Ca to the positive site and opening of the channel. Subsequently Ca will bind to the negative site, and this step has higher affinity than the previous one. The majority of channels opened will be closed after an initial period due to this high-affinity Ca binding at the negative site. Hence some channels that are opened by the initial stimulus will be closed by the same stimulus after a delay. This process gives rise to channel adaptation in the presence of constant Ca stimuli.

MATHEMATICAL MODEL OF CICR

In this section we propose a model based on independent Ca binding to the two regulatory sites on the ryanodine receptor. The state transition diagram is as follows.

$$\begin{array}{ccc} R & \underset{l_{-1}}{\overset{l_1}{\rightleftarrows}} & RC^+ \\ l_2 \Updownarrow l_{-2} & & l_2 \Updownarrow l_{-2} \\ RC^- & \underset{l_{-1}}{\overset{l_1}{\rightleftarrows}} & RC^+C^- \end{array} \tag{1}$$

Here R stands for the bare ryanodine receptor, C denotes cytosolic Ca, and C^+ (C^-) denotes the Ca bound to the positive (negative) regulatory site. Thus, RC^+ is the open state, and RC^+C^- is the closed state. The binding is independent in the sense that Ca binds to the positive or to the negative site with the same kinetic constants, irrespective of the state of the channel.

We first introduce the dimensionless variables $x_1 = [R]/[R]_T$, $x_2 = [RC^+]/[R]_T$, and $x_3 = [RC^+C^-]/[R]_T$, where $[R]_T$ denotes the total concentration of ryanodine receptors. From the conservation condition for receptors we have $[RC^-]/[R]_T = 1 - \sum_{i=1}^{3} x_i$. Let $x_4 = [\mathrm{Ca}]_i$ denote the Ca concentration in the cytoplasm. Then there are three differential equations for the channel kinetics:

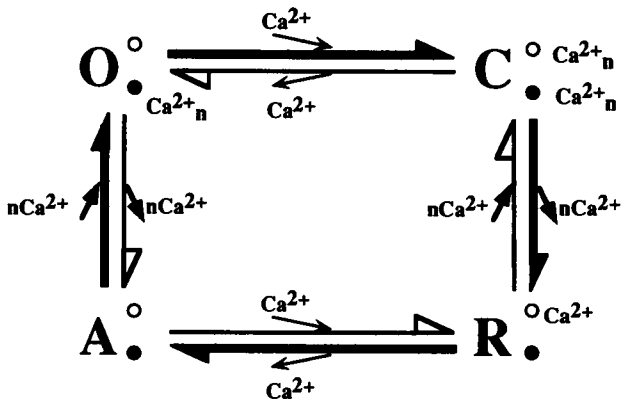

FIGURE 4 The model of RyR channel kinetics proposed in Fabiato (1992). The activating Ca binding site is represented by ●, the inactivating site by ○. O = open, C = closed, R = refractory, and A = activatable. The letter n before Ca or in subscript after Ca corresponds to the cooperative binding of several Ca ions.

$$\begin{aligned} \frac{dx_1}{dt} &= l_{-1}x_2 + l_{-2}\left(1 - \sum_{i=1}^{3} x_i\right) - (l_1 + l_2)x_1x_4 \\ \frac{dx_2}{dt} &= -l_{-1}x_2 + l_{-2}x_3 + (l_1x_1 - l_2x_2)x_4 \\ \frac{dx_3}{dt} &= -(l_{-2} + l_{-1})x_3 + \left(l_2x_2 + l_1\left(1 - \sum_{i=1}^{3} x_i\right)\right)x_4. \end{aligned} \tag{2}$$

The other components of the Ca dynamics are depicted in Fig. 1. An approach similar to that used in Othmer and Tang (1993) and Tang (1994) will be used to model these components. The flux due to the ATP-dependent pump that pumps cytosolic Ca back into the SR is given by

$$J_{p,SR} = \frac{p_1 x_4^2}{x_4^2 + p_2^2}. \tag{3}$$

Similarly, the pump on the sarcolemmal membrane that pumps cytosolic Ca into the extracellular medium produces the flux

$$J_{p,m} = \frac{q_1 x_4^2}{x_4^2 + q_2^2}. \tag{4}$$

In cardiac myocytes, voltage-dependent Ca channels in the sarcolemma are opened briefly after the onset of depolarization, and the resulting Ca influx is the primary trigger for further Ca release from internal stores. We model this influx by the term

$$J(t) = (H(t_{on}) - H(t - t_{off})) \cdot A_0 \tag{5}$$

where t_{on} and t_{off} are the on and off time of membrane depolarization, $H(t)$ is the unit step function, and A_0 is the amplitude of Ca influx in $[t_{on}, t_{off}]$. The open time $t_{off} - t_{on}$ for the sarcolemmal Ca channels will be taken as 250 ms in the following studies, while A_0 will be a variable parameter.

Since we have an external flux into the system, the total amount of Ca within the cytosol-SR complex is not conserved. An additional variable, $x_5 = [Ca]_{ER}$, has to be introduced to represent Ca concentration inside the SR. The Ca flux from the SR to the cytoplasm is proportional to the concentration of channels that are in the open state. The driving force for the flux is the Ca concentration gradient across the SR membrane. The channel-mediated Ca release is

$$J_{ch} = ch \cdot x_2(x_5 - x_4) \tag{6}$$

There are also leaks of Ca from the extracellular medium and the SR into the cytosol. Since we do not consider the electrical aspects in this study, the leakage rate of Ca across these membranes is assumed simply to be proportional to the concentration differences between the different compartments, i.e.,

$$J_{l,SR} = g_1(x_5 - x_4) \qquad J_{l,m} = g_2(C_0 - x_4). \tag{7}$$

Here C_0 stands for the extracellular Ca concentration, which is assumed to be a constant, and g_1 and g_2 are the leakage coefficients.

The additional equations for Ca dynamics in cardiac myocytes are

$$\begin{aligned}\frac{dx_4}{dt} &= v_r \cdot g_1(x_5 - x_4) + g_2(C_0 - x_4) - \frac{q_1 x_4^2}{x_4^2 + q_2^2} \\ &\quad + v_r\left(ch \cdot x_2(x_5 - x_4) - \frac{p_1 x_4^2}{x_4^2 + p_2^2}\right) + J(t) \\ \frac{dx_5}{dt} &= -g_1(x_5 - x_4) + \frac{p_1 x_4^2 - ch \cdot x_2(x_5 - x_4)}{x_4^2 + p_2^2}\end{aligned} \tag{8}$$

where v_r is the ratio of the SR volume to cytoplasmic volume, and $J(t)$ is specified influx. Table 1 contains the definition of parameters and the values used in this model.

ANALYSIS OF CHANNEL DYNAMICS

To study the RyR dynamics we must single out their effect from others, such as the effect of Ca pumps and the leakage in the SR and the sarcolemmal membrane. Experimentally this is difficult, since it involves isolating RyRs from myocytes and inserting them into lipid bilayers. However, it is easily done in the model: we only have to study Eq. 2 with x_4 as an externally given parameter.

TABLE 1 Parameter definitions and values

Location	Parameter	Value used	Definition
RyR channel	l_1	15 s^{-1} μM^{-1}	binding rate
	l_{-1}	7.6 s^{-1}	dissociation rate
	l_2	0.8 μM^{-1} s^{-1}	binding rate
	l_{-2}	0.84 s^{-1}	dissociation rate
	ch	80.0 s^{-1}	conductance
SR pump	p_1	1.038 × 10^3 μM s^{-1}	maximal rate
	p_2	0.12 μM	threshold concentration
Sarcolemma pump	q_1	19.0 μM s^{-1}	maximal rate
	q_2	0.06 μM	threshold concentration
Additional parameters	C_0	1.5 mM	extracellular Ca concentration
	v_r	0.185	volume ratio
	g_1	0.4 s^{-1}	leakage coefficient
	g_2	1.063 × 10^{-2} s^{-1}	leakage coefficient

Analysis of the steady state

In Eq. 2, the channel dynamics involves three equations. By setting the time derivatives equal to 0 we obtain

$$\begin{aligned} l_{-1}x_2 + l_{-2}\left(1 - \sum_{i=1}^{3} x_i\right) - (l_1 + l_2)x_1x_4 &= 0 \\ -l_{-1}x_2 + l_{-2}x_3 + (l_1x_1 - l_2x_2)x_4 &= 0 \\ -(l_{-2} + l_{-1})x_3 + \left(l_2x_2 + l_1\left(1 - \sum_{i=1}^{3} x_i\right)\right)x_4 &= 0. \end{aligned} \tag{9}$$

Since x_4 is fixed in these equations they can be solved uniquely for the fractions in the various states, and we find that the steady-state relationship between the fraction of open channels and stimulus Ca concentration is given by

$$x_2(x_4) = \frac{L_2 x_4}{L_1L_2 + (L_1 + L_2)x_4 + x_4^2}$$

where L_1 and L_2 are the dissociation constants, defined as $L_1 = (l_{-1}/l_1)$, $L_2 = (l_{-2}/l_2)$. x_2 is clearly a concave function of x_4 with a single maximum, and $x_2(0) = \lim_{x_4 \to \infty} x_2(x_4) = 0$. The maximum is reached at $x_4 = \sqrt{L_1L_2}$ and the maximum proportion of open channels in the steady state is $x_2 = L_2/(L_1 + L_2 + 2\sqrt{L_1L_2})$.

If we graph the fraction of channels open versus the logarithmic concentration of Ca, then we obtain the characteristic bell-shaped curve (Fig. 5). At low concentrations of cytosol Ca the steady-state fraction of channels open is low. As the Ca concentration increases the fraction of open channels reaches a maximum value, and for the parameter values in Table 1 this is around $[Ca]_i = 1$ μM, which is close to the value reported in Fabiato (1985) (Fig. 2). If the Ca concentration is increased beyond this value the fraction of open

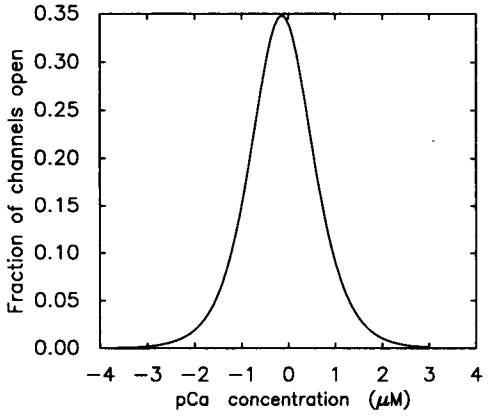

FIGURE 5 The fraction of channels open as a function of the Ca stimulus. The horizontal line represents the concentration of Ca in the cytosol. The vertical axis represents the proportion of channels in the open state at steady state.

channels decreases. The channels will be essentially completely closed at steady state when $[Ca]_i$ is in the mM range.

Adaptation of Ca channels in response to Ca stimuli

To simulate the adaptation experiment in Györke and Fill (1993) we will treat x_4 (the Ca concentration) as a parameter in Eq. 2. A step change in x_4 is applied to the system at $t = 0$, and the fraction of open channels computed as a function of time. The numerical output is shown in Fig. 6, where it is seen that adaptation of channel opening follows a step increase in Ca concentration. These results agree with the experimental results shown in Fig. 3.

The numerical simulations show that the adaptation is not complete. The unadapted portion at a given stimulus corresponds to the portion of channels open at steady state, which can be found by referring to the steady-state response curve in Fig. 5. For stimuli less than ~1 μM the unadapted fraction increases with increasing stimuli, but it decreases for stimuli greater than ~1 μM. Fig. 7 shows this fact and illustrates another prediction of the model: the rate of relaxation to the steady state increases as the stimulus increases. This can be understood from Eq. 2 when x_4 is held constant. This prediction is inconsistent with the claim made in Györke and Fill (1993), which states that the decay rate is independent of stimulus concentration. However, the range of Ca concentrations used in the experiment is very narrow. Should Györke and Fill perform the experiment with a much higher Ca concentration, they might be able to observe the increase in the relaxation rate predicted here.

LOCAL DYNAMICS OF THE INDEPENDENT-BINDING MODEL

Excitability and graded response

Cardiac myocytes have been regarded as a classical example of an excitable medium. Depolarization of the membrane opens the Ca channels and activates the Na/Ca exchanger in the sarcolemmal membrane. This induces an influx of Ca, which leads to contraction. However, the response is not all-or-none: one of the characteristics of this system is that the responses to nonsaturating stimulatory signals are graded (Stern, 1992). That is, the magnitude of the contraction is proportional to the magnitude of Ca entry from the extracellular medium after membrane depolarization (New and Trautwein, 1972). This observation is confirmed by measuring cytoplasmic Ca directly (Beuckelmann and Wier, 1988; Talo et al., 1990; Cleemann and Morad, 1990). It is now commonly believed that the amount of Ca released from the SR is proportional to the triggering Ca from the extracellular medium. There is also a threshold effect in E-C coupling, i.e., if the stimulus signal is smaller than a certain value, the signal cannot be amplified significantly.

As the following shows, the model displays these characteristics as well. If the stimulus A_0 in Eq. 5 is small, the response is small. When A_0 exceeds a threshold value the response becomes quite significant. Fig. 8 shows both a subthreshold response and a superthreshold response predicted by the model. The threshold value for significant amplification of the input signal is around 3.75 μM/s with $t_{off} - t_{on}$

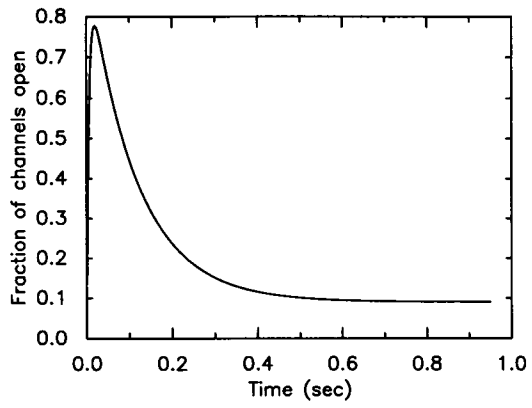

FIGURE 7 Adaptation of the channels at high Ca stimuli. Ca is raised from 0 to 10.0 μM at $t = 0$ and held constant thereafter.

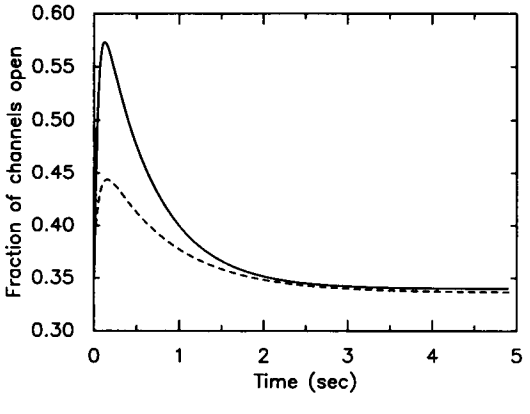

FIGURE 6 Numerical simulations of adaptation of channels to maintained stimuli. Ca is raised from 0 to 0.5 μM (----) or 1.0 μM (——) at $t = 0$ and held constant thereafter. Shown here are the time courses for the proportion of channels open in response to the step change in Ca.

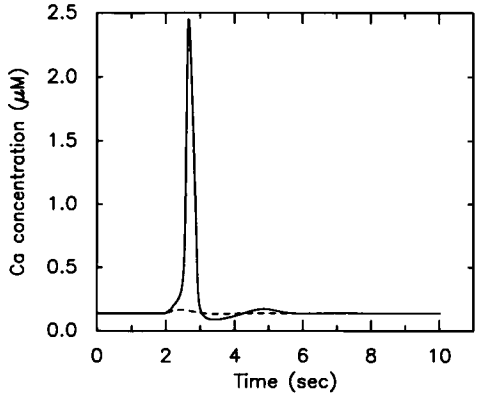

FIGURE 8 Excitability to Ca stimuli in the model. The stimuli are Ca influxes with amplitude 2.0 μM/s and 4.0 μM/s, respectively, for 250 ms. The response to 2.0 μM/s is subthreshold (dashed line), whereas to the stimulus of 4.0 μM/s is superthreshold. In the second case the contribution of the stimulus to the total increase in cytoplasmic Ca is insignificant.

= 250 ms. This threshold will decrease if the membrane is depolarized longer than 250- ms and increase if the depolarization is shorter, as would be expected from a threshold-duration relationship for an excitable medium.

Graded responses to graded stimuli are characterized more precisely as follows. When the membrane is depolarized to a fixed negative potential the cytoplasmic Ca increases, and for small depolarizations the steady-state level increases with the degree of depolarization. As the depolarization approaches the equilibrium potential of Ca the Ca current decreases, giving a typical bell-shaped curve for the relationship between membrane potential and maximal cytoplasmic Ca. In our model, numerical simulations reveal such graded responses over a wide range of inputs (cf. Fig. 9*a*). As the stimulus pulse increases in magnitude from 3.8 to 8.0 μM/s the peak value of cytoplasmic Ca increases from 2.5 to 4.0 μM. The graded response of cytoplasmic Ca to different stimuli can also be seen in the case of subthreshold responses, although to smaller amplitudes compared with responses in the case of superthreshold stimuli. In Fig. 9*b* a group of such responses is shown. In this figure one can see the initial Ca increase due to the Ca influx, but when the stimulus is withdrawn cytoplasmic Ca drops slightly, and then continues to increase.

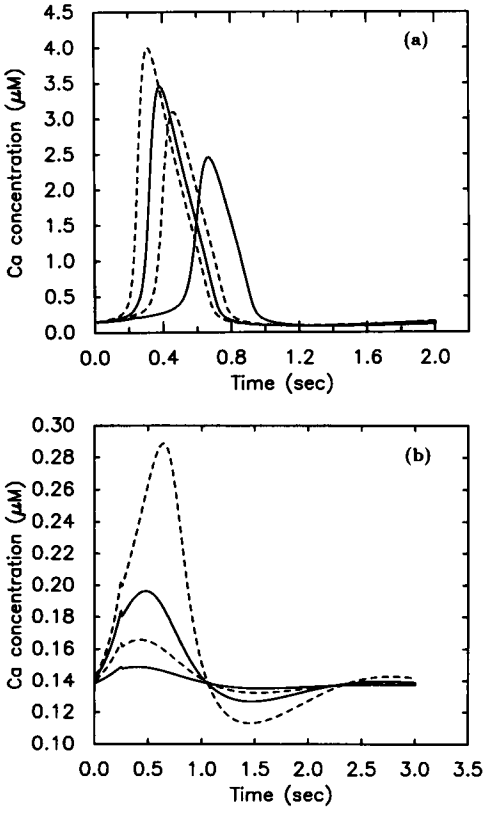

FIGURE 9 Graded cytoplasmic Ca responses to pulse Ca stimuli. The stimuli are constant Ca influxes for fixed time period and magnitude. Both the superthreshold response and subthreshold response show a graded response to stimuli of different magnitudes. In (*a*) the magnitudes are 4.0 μM/s, 5.0 μM/s, 6.0 μM/s, and 8.0 μM/s for $0 < t < 250$ ms. In (*b*) the magnitudes are 1.0 μM/s, 2.0 μM/s, 3.0 μM/s, and 3.7 μM/s for $0 < t < 250$ ms.

Another interesting aspect of the responses shown in Fig. 9*a* is the latency period between the onset of the stimulus and the occurrence of large excursions in the superthreshold responses. When the flux is 4.0 μM/s the large excursion of cytoplasmic Ca occurs ~400 ms after the onset of the stimulus. As the amplitude of the stimulus increases, the latency period gradually decreases to ~100 ms at the highest stimulus level (A_0 = 8.0 μM/s). These data correspond well with the experimentally observed results. In Talo et al. (1990) it is reported that the delay between the depolarization and the beginning of contraction ranges from 50 to 400 ms. When the membrane is depolarized to −40 mV the time delay is 300 ms, while this delay is reduced to ~50 ms when the membrane is depolarized to 0 mV.

A more direct test of the latency period can be designed as follows. In cardiac cells the major contribution to the initial Ca influx is from the voltage-sensitive Ca channel (the L-type Ca channels) (Bers, 1991). In the normal process of excitation the Ca current from this channel is sufficient to cause a rapid increase in cytoplasmic Ca, and there is no significant latency period. However, if we apply a drug to selectively block the L-type Ca channel (such as verapamil or nifedipine (Rousseau and Meissner, 1989)), then the amount of initial Ca entry from these channels decreases and the latency period before the onset of the intracellular Ca peak will gradually increase. Our prediction is that the cytoplasmic Ca profile should follow that of Fig. 9*a* as the drug concentration is increased. In very high concentrations of the drug no Ca increase will be measured, because the initial entry of Ca cannot reach the threshold value.

The model predicts another type of interesting dynamical behavior in response to very large Ca stimuli. If the stimulation level exceeds 9 μM/s two peaks of cytoplasmic Ca appear in response to the stimulus. This second peak has the same profile as the first peak, except that the peak Ca concentration is smaller. As the stimulus increases further more peaks may appear. Fig. 10 shows two cases of such responses for stimuli of 10.0 and 20.0 μM/s, respectively. Similar response profiles can be obtained by prolonging the pulse duration without increasing the pulse magnitude. These simulations can be tested by experiments using very high extracellular Ca concentration. Under this condition, a large pulse of Ca will enter the cell at depolarization. Similar behavior has been predicted for Ca dynamics controlled by $InsP_3$-sensitive channels (Othmer and Tang, 1993).

If the cytoplasmic Ca level is raised sufficiently by an initial injection of Ca the system shows damped oscillations. In this case the Ca cannot be pumped out of the cell rapidly enough by the membrane Ca pumps and the Na/Ca exchanger. The lowest level of cytoplasmic Ca after the first peak is raised, which brings the system into oscillatory mode. When the dynamics are tuned properly this can occur for several cycles. However, the oscillation disappears after the excess Ca is pumped out of the cell. The steady state of the system is independent of the initial stimulus, and thus the system eventually returns to its prestimulus steady state. Although we do not know of examples in which this behavior

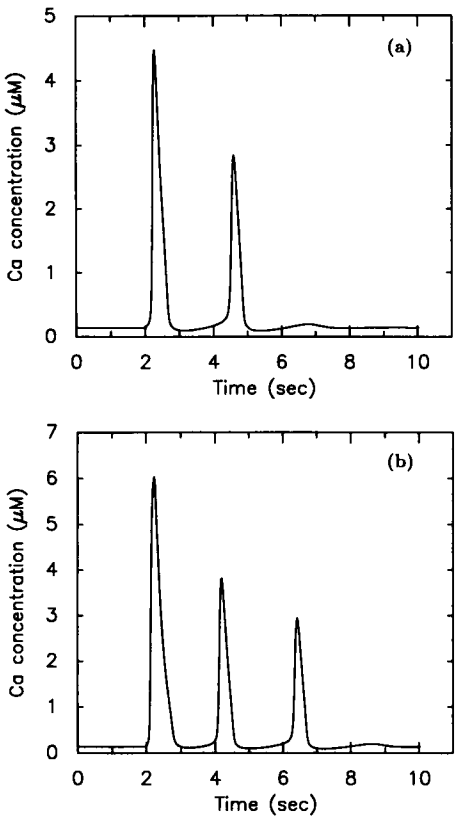

FIGURE 10 Ca dynamics in overstimulated cases. When the influx exceeds 9.0 μ/s for 250 ms duration a secondary response or a sequence of Ca bursts results. (*a*) $J_{(t)} = 10.0$ μM/s, 2.0 s < t < 2.25 s; (*b*) $J(t)_{flux} = 20.0$ μM/s, 2.0 s < t < 2.5 s.

has been observed in experiments, the phenomenon of triggered depolarization provides indirect support for this type of behavior.

Triggered depolarization, or afterpolarization, involves several delayed depolarizations that occur after the cell has repolarized (Katz, 1992). It has been suggested that the afterpolarization in cardiac cells is due to Ca oscillations within the cell after a depolarization, since it usually occurs in a Ca-overloaded heart. We can understand the afterpolarization in several ways. For example, elevated Ca in the blood or a prolonged membrane depolarization leads to a large influx of Ca into the cell. As we argued above, it can happen that such large dosages of Ca cannot be cleared out sufficiently rapidly, and a Ca oscillation is induced. This Ca oscillation can give rise to partial membrane depolarization, since Ca release from the SR alters the membrane permeability to electrolytes and the electrical balance in the cell. Other pathologies that cause the temporal accumulation of extra Ca in cytosol-SR system can also give rise to afterpolarizations.

Oscillations

Cardiac cells can also become self-oscillatory under various conditions (Wier and Blatter, 1991; Kort and Lakatta, 1984; Kort et al., 1985). One way to induce oscillations is to increase the conductance for the leakage from the extracellular medium into the cytoplasm, which can result, e.g., from physical damage to the sarcolemmal membrane. When this occurs cytoplasmic Ca concentration can show sustained oscillations in the normal range of extracellular Ca. The oscillatory cells respond to a further increase in extracellular Ca with an increased frequency of oscillation (Glisch and Pott, 1975; Fabiato, 1983; Fabiato, 1983; Capogrossi and Lakatta, 1985), i.e., they show a form of frequency encoding. As the leakage rate of extracellular Ca increases in our model, the cell becomes self-oscillatory without any other changes, just as in the experiments. An example of the oscillation is shown in Fig. 11. Contrary to the common belief that this oscillation is induced by spontaneous release of Ca due to overload of the SR (Fabiato, 1985; Wier and Blatter, 1991), the oscillation in the model is triggered by the increase in the steady-state Ca concentration in the cytosol that results from the increased leakage. Numerical simulation also shows an increase in the oscillation frequency and amplitude as the extracellular Ca concentration increases (Fig. 12).

The simulations show that cells are very sensitive to increases in the coefficient for the sarcolemmal leakage. Oscillations ensue at $g_2 = 1.09 \times 10^{-2}$, and as the leakage coefficient increases further, both the oscillation frequency

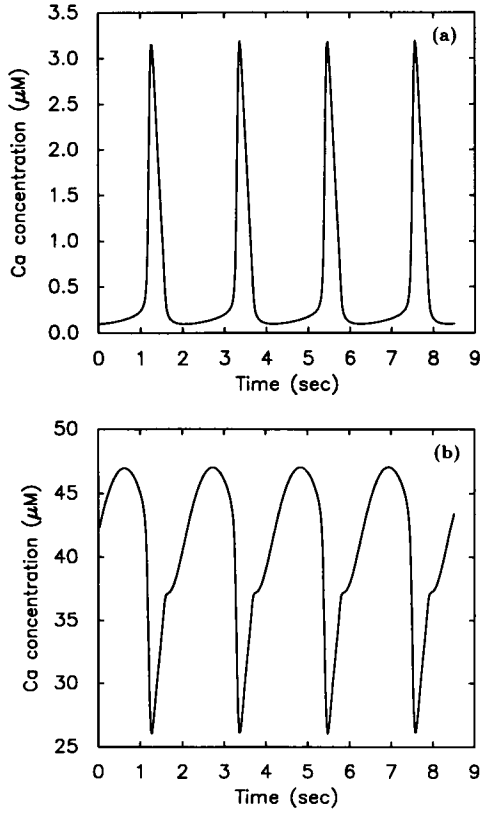

FIGURE 11 Cardiac cells become self-oscillatory as either the leakage coefficient g_2 or the extracellular Ca concentration increases sufficiently. (*a*) Cytoplasm. (*b*) Sarcoplasmic reticulum. In the numerical simulation shown here g_2 is increased from 1.063×10^{-2} to 1.093×10^{-2}.

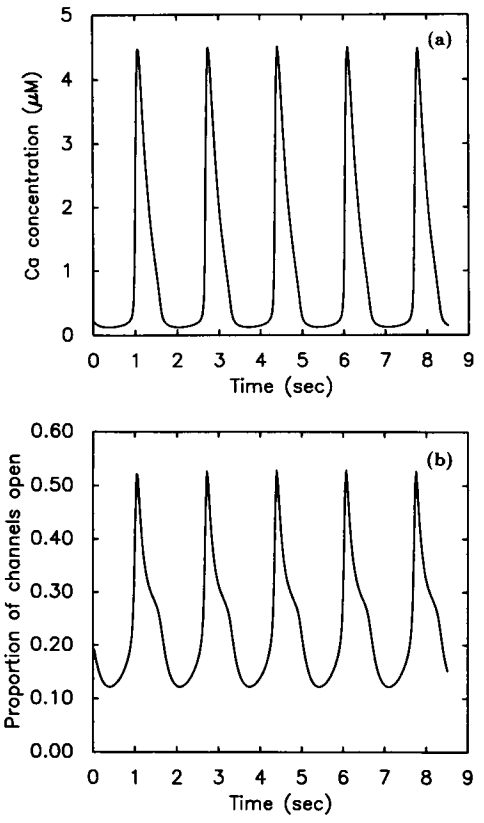

FIGURE 12 The oscillation frequency increases as the extracellular Ca concentration increases. (*a*) Cytoplasm Ca. (*b*) Channel open. The leakage coefficient is the same as in Fig. 11, but the extracellular Ca concentration is increased from 1.5 to 1.6 mM. The period in Fig. 11 is 2.0 s and the period here is 1.5 s.

and amplitude increase (similar to the effect of increasing extracellular Ca shown in Fig. 12). If g_2 increases beyond 1.25×10^{-2} the oscillation disappears and the system remains at a high value of the steady-state cytoplasmic Ca (result not shown). If the leakage rate increases enough to exceed the pump capacities ($g_2 > 1.3 \times 10^{-2}$) there is no steady state; Ca simply increases. Increasing the extracellular Ca to very high levels has a similar effect on oscillations in cells. Namely, the system passes through an oscillatory regime in which the oscillation frequency increases, but eventually the oscillations are replaced by a high level of steady-state cytoplasmic Ca. At sufficiently high extracellular Ca the cell cannot control the cytoplasmic Ca (Stern et al., 1988). The reason for this similarity between an increase in the leakage coefficient and the extracellular Ca is easy to understand mathematically, since the leakage rate is determined by $g_2(C_0 - x_4)$.

Other changes in the parameter values can also result in oscillations. For example, Ca oscillations can occur when the ATP concentration is low. We model this condition by a decrease in the maximal pumping rate for the pump in the sarcolemmal membrane. This decrease in the maximal rate (q_1) results in Ca accumulation in the cytosol, which brings the system into the oscillatory mode (Fig. 13). Such oscillations have been observed experimentally in certain cells under conditions of energy depletion (Orchard et al., 1983). In coupled arrays of cells a secondary electrical signal due to the Ca oscillation in one cell may cause the depolarization of neighboring cells and hence start a local oscillation (an ectopic focus), which interferes with the normal functioning of the cell population.

Experimentally, addition of caffeine can also cause a quiescent cell to oscillate or it can increase the oscillation frequency of oscillatory cells (Capogrossi et al., 1984). We model this effect by an increase in the Ca channel conductance (*ch*), as is suggested in Meissner and El-Hashem (1992). This increase in *ch* can either bring a quiescent cell into the oscillatory range or increase the frequency of the oscillation in an oscillatory cell. The reason for this response is clear: increasing *ch* causes an increase in cytosolic Ca, as in the case of an increase of the leakage rate, and the oscillations are very similar in the two cases (cf. Figs. 11 and 12).

TRAVELING CA WAVES IN CARDIAC CELLS

Traveling waves in a single cardiac cell were first observed as waves of contraction (Kort et al., 1985). As the techniques for monitoring Ca in a cell by fluorescent microscopy developed, traveling Ca waves in single cardiac cells could also be observed (Takamatsu and Wier, 1990; Williams et al., 1992). A traveling Ca wave usually starts from one end of the cell and travels the entire length of the cell. When two independent waves are initiated from separate ends, the waves meet and annihilate in the interior. Other types of wave phenomena have also been observed, such as a wave train starting from one end or a wave initiating from a central point in the cell and radiating outward as a target pattern (Williams et al., 1992).

Traveling Ca waves can be initiated where local damage to the sarcolemmal membrane causes a local increase in the Ca flux. However, waves are usually initiated from the ends of a cell, and there are several reasons for this: 1) the damage to the sarcolemmal membrane usually occurs there; 2) the channel density is usually higher at the ends of the SR close

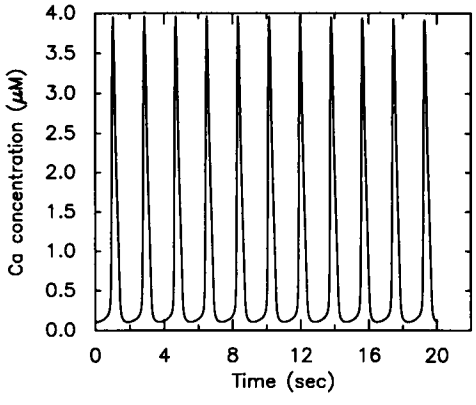

FIGURE 13 Oscillations due to a decrease in q_1, which is decreased from 19 to 18 μM/s.

to the membrane; and 3) the end points have a high surface-to-volume ratio, giving rise to locally higher Ca entry even without membrane damage. These factors contribute to the hypersensitivity to Ca perturbations at the ends. Once such a perturbation exceeds the threshold for initiation of the positive feedback mechanism that underlies CICR, a local burst of Ca occurs. Such a burst diffuses and causes the neighboring channels to open, and in this way a traveling wave is initiated. However, Ca waves do not only initiate from the ends (Williams et al., 1992); any factor that can cause a local increase of Ca to the threshold value can initiate a Ca wave.

In the following model we will assume that the distributions of Ca channels and pumps are spatially uniform. This assumption makes the ends of the cell equally sensitive to a Ca stimulus as any other part of the cell. In reality the SR Ca stores are composed of small individual subunits that are separate from each other (Oldershaw et al., 1991), but in the continuum description adopted here we treat them as uniformly distributed in space. In essence, our model is a two-phase continuum description. The dynamics of the channels and the SR calcium are unchanged, and the governing equation for cytosolic Ca is

$$\frac{\partial x_4}{\partial t} = D_{CA}\frac{\partial^2 x_4}{\partial z^2} + v_r \cdot g_1(x_5 - x_4) + g_2(C_0 - x_4) - \frac{q_1 x_4^2}{x_4^2 + q_2^2} + v_r\left(ch \cdot x_2(x_5 - x_4) - \frac{p_1 x_4^2}{x_4^2 + p_2^2}\right) + J(z, t) \qquad (10)$$

$$\left.\frac{\partial x_4}{\partial z}\right|_{z=0} = \left.\frac{\partial x_4}{\partial z}\right|_{z=l} = 0.$$

Here D_{CA} is the diffusion coefficient of Ca, which we set at 5.0×10^{-4} mm^2/s. z denotes the unscaled position along the cell ($0 < z < l$) where l is the cell length. To initiate a traveling wave, a local superthreshold source of Ca flux is applied to the cytoplasm for a short period. The imposed influx term, which is also a function of time, is denoted $J(z, t)$. The amplitude of influx actually must be slightly higher than the threshold for the local dynamics to initiate a traveling wave, since the Ca diffusion can reduce the effective stimulus at the location. The Neumann boundary condition simply means no Ca can diffuse across the ends of the cell.

A traveling wave obtained from numerical simulation is shown in Fig. 14. The time profile of the wave is shown at $z_1 = 10$ μm, $z_2 = 50$ μm, $z_3 = 75$ μm, and $z_4 = 100$ μm. At $z = 10$ μm, where the stimulus is imposed, there is a 200-ms latent period before a large burst of Ca appears, which then begins to travel. At $z = 10$ μm, Ca reaches a maximum concentration of 2.5 μM. As it travels along the cell the peak Ca level decreases slightly and stabilizes at about 2.0 μM for $z = z_2$ and $z = z_3$. At the right boundary point ($z = 100$ μm) Ca reaches a maximum value of about 3.7 μM. The Ca at the right end exceeds the maximum levels in the interior because there is reflection of the Ca wave at the boundary.

The wave speed is about 81 μm/s in Fig. 14, which is much faster than was found in a model for calcium dynamics con-

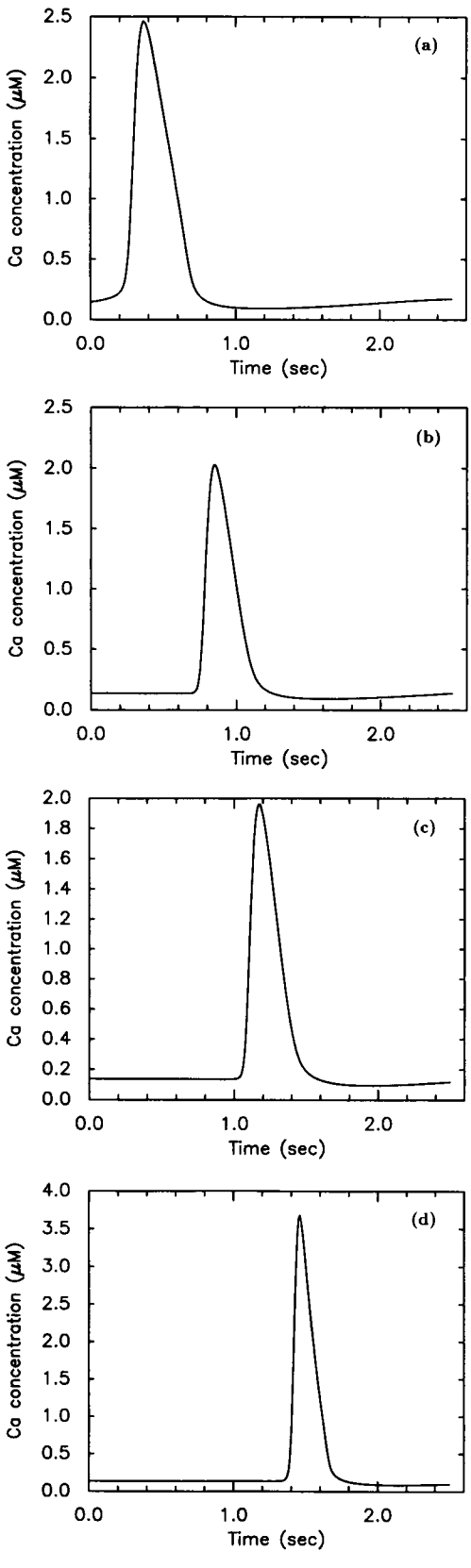

FIGURE 14 A one-dimensional traveling wave viewed at different locations within a cell. The wave is initiated at the left end of the cell and travels toward the right. $J(z, t) = 8.0$ μM/s for $0 < t < 0.25$ s, and $0 < z < 10$ μm and $J(z, t) = 0$ elsewhere. The length of the interval is 100 μm. (*a*) $z_1 = 10$ μm; (*b*) $z_2 = 50$ μm; (*c*) $z_1 = 75$ μm; (*d*) $z_2 = 100$ μm.

trolled by IP_3-sensitive channels (Othmer and Tang, 1993). The increase in speed is not due to differences in the diffusion coefficient, but rather to the channel dynamics, which produces a sharper traveling front in the present case. The wave speed increases if we increase the extracellular Ca concentration or increase the leakage rate g_2. Typical speeds for experimentally observed cardiac Ca waves are ~100 μm/s at 21°C (Wier and Blatter, 1991). For other experiments speeds in the range of 50–150 μm/s have been reported (Williams et al., 1992).

Fig. 15 shows experimental results on how two waves initiated from the ends of the cell propagate and annihilate where they meet. Fig. 16 is a numerical simulation of the corresponding process. The numerical images in this case are generated by fixing the time and plotting the Ca profile at that time. The wave traveling to the right is started by a flux of magnitude $A_0 = 8$ μM/s, and the one traveling to the left by a flux with $A_0 = 6$ μM/s. Although the stimuli are imposed at the same time, the wave traveling to the right starts to propagate sooner than the wave traveling to the left (t = 0.5 s). The delay in the initiation of the latter is due to the longer latent period associated with the smaller influx of Ca. At time $t = 1.0$ s the two waves have settled down to a fixed amplitude of about 2.0 μM, although the initial height of Ca is different. The two wave fronts meet and annihilate at about 76 μm. Annihilation of the waves occurs because there is a refractory period before the medium becomes excitable again. A high Ca level is reached at the moment of collision of the two waves ($t = 1.25$ s), as is seen in the experiments. After collision, both waves disappear ($t = 1.5$ s).

Traveling waves can also be initiated at other locations in the cell. In Fig. 17 a traveling wave is started from the center of the domain. This wave can be initiated by short-term damage to the membrane at this location, which leads to a larger influx of Ca at this point as compared with other points. If the local damage is not instantaneous, but long lasting, then a constant elevation of the Ca influx results. This elevated influx can induce a sequence of traveling waves, which propagate in both directions in the numerical simulation (result not shown).

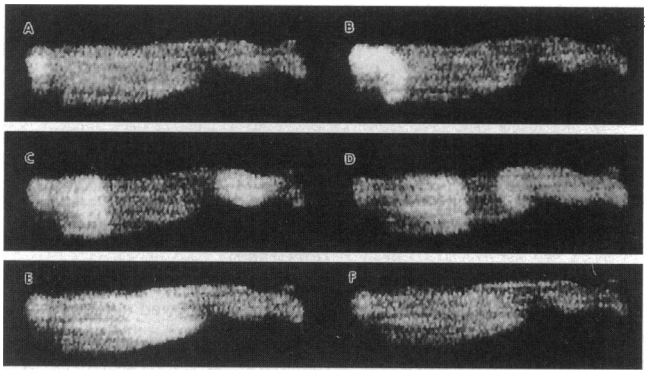

FIGURE 15 An experimental result that shows interacting waves. The cell length is 143 μm. Taken from Williams et al. (1992) with permission.

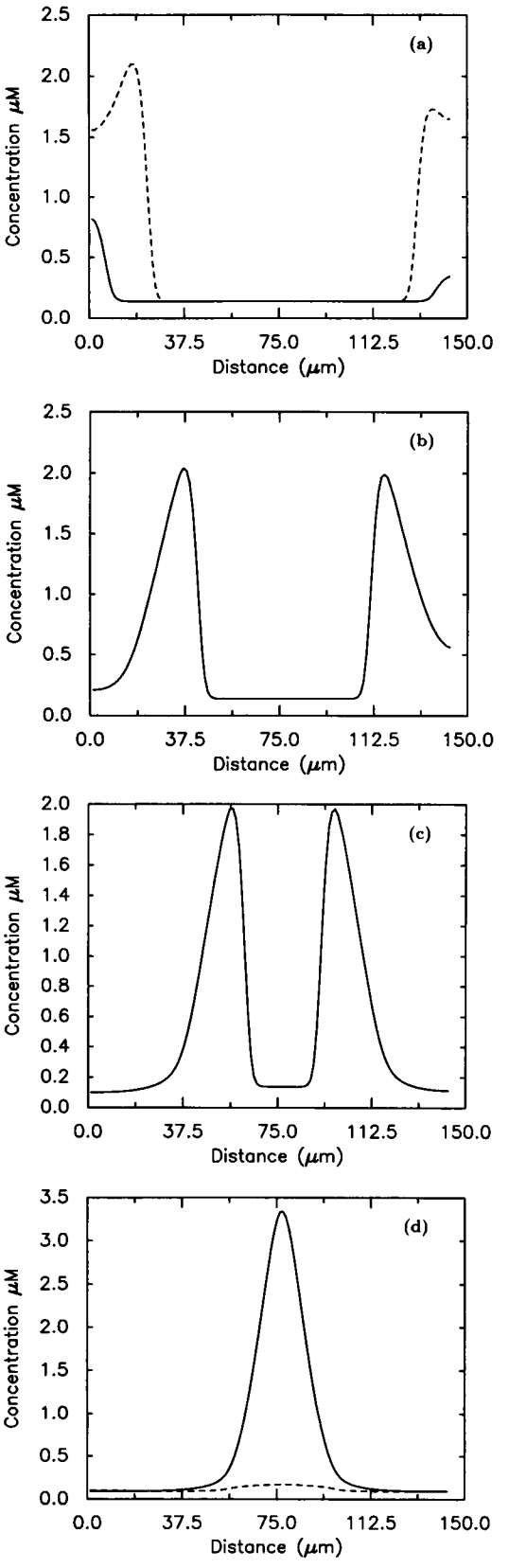

FIGURE 16 The spatial profile of Ca in interacting waves computed in a numerical simulation. The cell length is 143 μm as in Fig. 15. The Ca concentration is shown here at fixed times. In case an x-profile is drawn at two different times, the later one is depicted by a dashed line and the earlier one by a solid line. (a) $t_1 = 0.25$ s and $t_2 = 0.5$ s; (b) $t_3 = 0.75$ s; (c) $t_4 = 1.0$ s; (d) $t_5 = 1.25$ s and $t_6 = 1.50$ s.

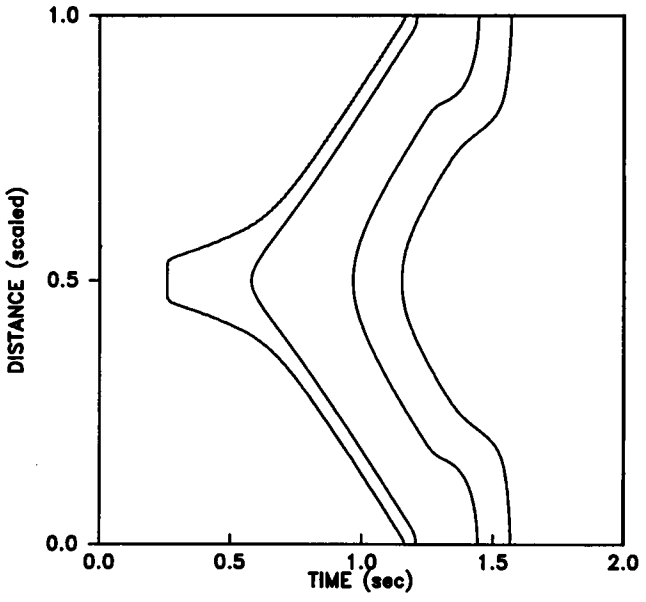

FIGURE 17 A space-time plot of a traveling wave initiated from the center. The wave is initiated by a Ca in flux of magnitude 8 μM/s for 250 ms < t < 500 ms. The cell length is 100 μm.

DISCUSSION

Summary

We have developed a model for the ryanodine-sensitive Ca channels in this paper. The model is based on the assumptions that there are two regulatory Ca binding sites on the channel complex, one positive and the other negative, and that the binding of Ca to the two sites is independent. The model exhibits both the static and dynamic behavior seen in experiments. This includes the bell-shaped fraction of channels open as a function of pCa at steady state and adaptation in time to step increases in Ca stimulus. The channel model is then incorporated in a model for Ca dynamics in cardiac myocytes. The Ca conductance from the SR to the cytoplasm is assumed to be a linear function of the fraction of open channels. The other components of the model include Ca leakage terms across the SR membrane and sarcolemmal membrane. There are also Ca pumps in the SR membrane and in the sarcolemmal membrane. The Ca entry from the extracellular medium after depolarization is modeled by a square pulse of 250 ms duration and varying amplitude.

The model can reproduce the observed phenomena for whole-cell preparations, including excitability and smoothly graded responses to stimuli at both super- and subthreshold values. Under various pathological conditions, such as a leaky membrane, addition of caffeine, or low cytoplasmic ATP concentration, the system becomes oscillatory. The oscillatory cells respond to an increase in the extracellular Ca concentration by increasing the oscillation frequency and amplitude.

When a spatially distributed version of the model is studied in one space dimension, it predicts traveling Ca waves that can be initiated by a pulse application of Ca at fixed locations. Once initiated, they travel with a speed of about 80 μm/s and a maximum Ca concentration of $\sim$2 μM, which are in the experimental range. The wave speed and the maximal amplitude can be modified by changing the extracellular Ca concentration or the leakage rate, but not by changing the initiating stimulus. When Ca waves are initiated from both ends of a cell they annihilate when they meet. When there is a continuous Ca influx at one point, trains of Ca waves are initiated from this point. Extension of this model to two space dimensions will produce target patterns or spiral waves depending on the specific geometry of the given cell and the initial stimulus (Lipp and Niggli, 1993).

Other possible models for the channel kinetics

In reality the binding of regulatory factors may be not completely independent, as is proposed in this model. Instead, the binding and unbinding of cytosolic Ca to the regulatory sites on the channel can be state dependent. To account for such state-dependent binding and unbinding of regulatory factors, a new scheme has to be introduced, as shown in Eq. 11. This scheme is similar to that for the independent model, but more kinetic constants are involved.

$$\begin{array}{ccc} R & \underset{l_{-1}}{\overset{l_1}{\rightleftarrows}} & RC^+ \\ l_4 \Updownarrow l_{-4} & & l_2 \Updownarrow l_{-2} \\ RC^- & \underset{l_{-3}}{\overset{l_3}{\rightleftarrows}} & RC^+C^- \end{array} \tag{11}$$

The independent-binding model can be viewed as a special case of this model in which $l_3 = l_1$, $l_4 = l_2$, $l_{-3} = l_{-1}$, and $l_{-4} = l_{-2}$. However, since there are more independent parameters involved here, this new scheme has more degrees of freedom to accommodate various experimental results, provided the parameters can be estimated.

An even simpler model than is used here results by choosing $l_3 = l_{-3} = l_4 = l_{-4} = 0$. In this case the kinetic scheme is

$$\begin{array}{c} R + C \underset{l_{-1}}{\overset{l_1}{\rightleftarrows}} RC^+ \\ RC^+ + C \underset{l_{-2}}{\overset{l_2}{\rightleftarrows}} RC^+C^- \end{array} \tag{12}$$

The model is sequential-binding in the sense that Ca can only bind to the negative site after binding to the positive site, and also in the sense that the Ca in the negative site has to be released before the Ca in the positive site can be released from the channel. This model shows the same type of characteristics as the independent-binding model at the channel level (unpublished results). In the local dynamics, both the sequential-binding and the independent-binding models can behave as excitable media and can become oscillatory under similar circumstances. When the spatial aspect is introduced, they both have stable traveling wave solutions. The sequential model is better suited for theoretical analysis, since the system has fewer variables. With simplifications, the sequential-binding model can be reduced to only two equa-

tions, and one can prove the existence of traveling wave solutions (unpublished result). The independent-binding model involves one more variable than the sequential-binding model to account for the additional channel state RC^-. It also matches the model proposed by Fabiato (1992).

Relation to previous models

There is extensive literature on mathematical models of Ca dynamics (Keizer, 1993). Roughly, these papers can be divided into three categories depending on the type of Ca channels involved: 1) those with IP_3-sensitive Ca channels (IP_3R) only (De Young and Keizer, 1992; Othmer and Tang, 1993); 2) those with ryanodine-sensitive Ca channels only (Stern et al., 1988); Wong et al., 1992); and those involving both types of channels (Goldbeter et al., 1990; Dupont et al., 1991). We will discuss only those in the above categories that are relevant to the models presented here.

De Young and Keizer (1992) first proposed a mathematical model based on the dynamics of IP_3R. In this model, it is proposed that the IP_3Rs are regulated by cytoplasmic Ca both positively and negatively, similar to the model proposed by Fabiato (1992). In addition, there is an additional IP_3-regulatory site that up-regulates the channel conductivity upon IP_3 binding. The binding of different regulatory factors (Ca and IP_3) to the channel is assumed to be state dependent. Othmer and Tang (1993) later proposed a model with simpler channel kinetics, in which the binding of regulatory factors is assumed to be sequential. The mathematical merit of this model is that it contains fewer variables and hence is more amenable to analysis. Which of these two models better represents reality has to be determined by further experimental studies on the channel complex.

Biochemically, the similarity between RyR and IP_3R is very striking. They both have a similar fourfold pinwheel shape. Ca has both positive and negative regulatory effects on these channels (Bezprozvanny et al., 1991). The cooperativity of channel opening found in both of these two types is further evidence supporting their functional similarity. This similarity is the basis for developing models for RyR similar to those for IP_3R. The state dependent and sequential models for RyR developed here correspond to the state dependent binding model and sequential model for IP_3R in De Young and Keizer (1992) and Othmer and Tang (1993).

Understanding Ca dynamics in cardiac myocytes is important for a variety of reasons, and there have been previous models developed for this purpose. A mathematical model for CICR in cardiac cells that did not use the channel kinetics proposed by Fabiato (1992) was developed by Wong et al. (1992). These authors used a Hodgkin-Huxley type of channel kinetics with the gating mechanism determined by cytoplasmic Ca. In the model, the RyR channel kinetics involves the faster activation and slow inhibition through the gating event. The model can simulate experimental data of skinned cardiac muscle preparations, as well as the whole-cell preparations. Since the model proposed in Wong et al. (1992) involves many more compartments than the simple models presented here, it is hard to compare them directly. Li and Rinzel (1994) have shown recently that the channel kinetics in the De Young-Keizer model can be reduced to a Hodgkin-Huxley form. It is conceivable that the same argument may be applied to the models presented here, in which case a more direct comparison can be made with the model in Wong et al. (1992).

Stern (1992) has also developed a class of Ca dynamics models for cardiac myocytes. Although each model can simulate a specific event in cardiac myocytes, no single model can satisfactorily explain all the aspects of Ca dynamics in cardiac myocytes. The essential difficulty is to account for the graded Ca releases from SR in response to graded Ca stimuli. Based on the assumption that Ca release is a linear function of the Ca stimulus, Stern shows that no common-pool model (see Stern (1992) for the definition) can account for the graded Ca release from the SR. The linearity assumption is based on the experimental observations on Ca channels incorporated into lipid bilayers (Rousseau and Meissner, 1989; Ashley and Williams, 1990). These results are inconsistent with the fact that high cytoplasmic Ca has an inhibitory effect on the open channels in skinned muscle preparations (Fabiato, 1985, 1992). One possible explanation is that the experimental manipulations involved in isolating and incorporating Ca channels in a bilayer may affect their behavior. Another possibility is that certain cytoplasmic factors must be present for the inhibitory effect of Ca on RyR to be manifested.

Although the models proposed in this paper fall into the category of "common-pool" models, the relationship between the stimulus Ca and Ca release from the SR is definitely nonlinear. Hence the linear analysis for the models in Stern (1992) is not applicable in this case. In addition, our model shows graded Ca release from the SR in response to pulse Ca stimuli. This graded Ca release is coupled to the threshold effect of an excitable medium. There is a quasi-linear relationship between triggering Ca and the resulting Ca concentration below or above the threshold. Around the threshold value small changes in the amplitudes of the stimulus are capable of producing very large differences in response. The threshold effect corresponds to the onset of a region of rapid increase in the triggered Ca release curve as a function of depolarizing signal (between -40 and -10 mV) (Cannell et al., 1987; Beuckelmann and Wier, 1988).

There are other models that are not primarily designed for modeling CICR but they include CICR as an ingredient; such models include the collection of models proposed by Harrison et al. (1992) and Goldbeter et al. (Dupont et al., 1991; Goldbeter et al., 1990). The modeling of the channel kinetics in all these models is of the quasi-steady Michaelis-Menton type. Although the expression accounts for the fact that the cytosolic Ca concentration has a positive effect on the Ca release, it does not account for the negative effect of high Ca concentrations on the Ca release. Most importantly, it does not incorporate the different time course of channel kinetics in response to cytoplasmic Ca changes.

Kenneth W. Spitzer and Timothy J. Lewis provided us with much information and fruitful discussions during the development of the model presented here. We thank John Stephenson for his critical suggestions for the revision of this work. This research is supported in part by National Institutes of Health grant GM 29123.

REFERENCES

Ashley, R., and A. Williams. 1990. Divalent cation activition and inhibition of single calcium release channels from sheep cardiac sarcoplasmic reticulum. *J. Gen. Physiol.* 95:981–1005.

Bers, D. 1991. Excitation-contraction Coupling and Cardiac Contractile Force. Kluwer Academic Publishers, London, UK. 247 pp.

Beuckelmann, D., and W. Wier. 1988. Mechanism of release of calcium from sarcoplasmic reticulum of guinea-pig cardiac cells. *J. Physiol.* 405: 233–255.

Bezprozvanny, I., J. Watras, and B. Ehrlich. 1991. Bell-shaped calcium-response curves of Ins(1,4,5)P_3- and calcium-gated channels from endoplasmic reticulum of cerebellum. *Nature.* 351:751–754.

Cannell, M., J. Berlin, and W. Lederer. 1987. Effect of membrane potential changes on the calcium transient in single rat cardiac muscle cells. *Science.* 238:1419–1422.

Capogrossi, M., A. Fraticelli, and E. Lakatta. 1984. Ca^{2+} release from the sarcoplasmic reticulum: different effects of ryanodine and caffeine (abstract). *Fed. Proc.* 43:820.

Capogrossi, M., and E. Lakatta. 1985. Frequency modulation and synchronization of spontaneous oscillations in cardiac cells. *Am. J. Physiol.* 248: H412–H418.

Cleemann, L., and M. Morad. 1990. Role of Ca^{2+} channel in cardiac excitation-contraction coupling in the rat: evidence from Ca^{2+} transients and contraction. *J. Physiol.* 432:283–312.

De Young, G. and J. Keizer. 1992. A single pool IP_3-receptor-based model for agonist stimulated Ca^{2+} oscillations. *Proc. Natl. Acad. Sci. USA.* 89: 9895–9899.

Dupont, G., M. Berridge, and A. Goldbeter. 1991. Signal-induced Ca oscillations: properties of a model based on Ca-induced Ca release. *Cell Calcium.* 12:73–85.

Fabiato, A. 1983. Calcium-induced release of calcium from the cardiac sarcoplasmic reticulum. *Am. J. Physiol.* 245:C1–C14.

Fabiato, A. 1985. Time and calcium dependence of activation and inactivation of calcium-induced release of calcium from the sarcoplasmic reticulum of a skinned canine cardiac Purkinje cell. *J. Gen. Physiol.* 85: 247–289.

Fabiato, A. 1992. Two kinds of calcium-induced release of calcium from the sarcoplasmic reticulum of skinned cardiac cells. *In* Excitation-Contraction Coupling in Skeletal, Cardiac, and Smooth Muscle. G. B. G. Frank, P. Bianchi, and H. Keurs, editors. New York: Plenum Press. 245–263.

Glisch, H., and L. Pott. 1975. Spontaneous tension oscillations in guinea-pig atrial trabeculae. *Pflugers Arch.* 358:11–25.

Goldbeter, A., G. Dupont, and M. Berridge. 1990. Minimal model for signal-induced Ca oscillations and for their frequency encoding through protein phosphorylation. *Proc. Natl. Acad. Sci. USA.* 87:1461–1465.

Györke, S., and M. Fill. 1993. Ryanodine receptor adaptation: control mechanism of Ca^{2+}-induced Ca^{2+} release in heart. *Science.* 260:807–809.

Harrison, S., E. McCall, and M. Boyett. 1992. The relationship between contraction and intracellular sodium in rat and guinea-pig ventricular myocytes. *J. Physiol.* 449:517–550.

Katz, A. 1992. Physiology of the Heart, 2nd ed. Raven Press, New York. 687 pp.

Keizer, J. 1993. Calcium oscillations and waves: is the IP_3R Ca^{2+} channel the culprit? *Biophys. J.* 65:1359–1361.

Kort, A., M. Capogrossi, and E. Lakatta. 1985. Frequency, amplitude, and propagation velocity of spontaneous Ca^{++}-dependent contractile waves in intact adult rat cardiac muscle and isolated myocytes. *Circ. Res.* 57: 844–855.

Kort, A., and E. Lakatta. 1984. Calcium-dependent mechanical oscillations occur spontantaneously in unstimulated mammalian cardiac tissues. *Circ. Res.* 54:396–404.

Lai, A., M. Misra, L. Xu, A. Smith, and G. Meissner. 1989. The ryanodine receptor-Ca^{2+} release channel complex of skeletal muscle sarcoplasmic reticulum. *J. Biol. Chem.* 264:16776–16785.

Li, Y., and J. Rinzel. 1994. Equations for $InsP_3$ receptor-mediated $[Ca^{2+}]_i$ oscillations derived from a detailed kinetic model: a Hodgkin-Huxley like formalism. *J. Theor. Biol.* In press.

Lipp, P., and E. Niggli. 1993. Microscopic spiral waves reveal positive feedback in subcellular calcium signaling. *Biophys. J.* 65:2272–2276.

Liu, Q., A. Lai, E. Rousseau, R. Jones, and G. Meissner. 1989. Multiple conductance states of the purified calcium release channel complex from skeletal sarcoplasmic reticulum. *Biophys. J.* 55:415–424.

Meissner, G., and A. El-Hashem. 1992. Ryanodine as a functional probe of the skeletal muscle sarcoplasmic reticulum Ca^{2+} release channel. *Mol. Cell. Biochem.* 114:119–123.

Meissner, G., F. Lai, K. Anderson, L. Xu, Q. Liu, A. Herrmann-Frank, E. Rousseau, R. Jones, and H. Lee. 1991. Purification and reconstruction of the ryanodine- and caffeine-sensitive Ca^{2+} release channel complex from muscle sarcoplasmic reticulum. *In* Regulation of Smooth Muscle Contraction. R.S. Moreland, editor. Plenum Press, New York. 241–256.

New, W., and W. Trautwein. 1972. The ionic nature of slow inward current and its relation to contraction. *Pflugers Arch.* 334:24–38.

Orchard, C., D. Eisner, and D. Allen. 1983. Oscillations of intracellular Ca^{2+} in mammalian cardiac muscle. *Nature.* 304:735–738.

Oldershaw, N., D. Nunn, and C. Taylor. 1991. Quantal Ca^{2+} mobilization stimulated by inositol 1,4,5-trisphosphate in permeabilized hepatocytes. *Biochem. J.* 278:705–708.

Othmer, H., and Y. Tang. 1993. Oscillations and waves in a model of calcium dynamics. *In* Experimental and Theoretical Advances in Biological Pattern Formation. H. Othmer, p. Maini, and J. Murray, editors. Plenum Press, London, UK.

Rousseau, E., and G. Meissner. 1989. Single cardiac sarcoplasmic reticulum Ca^{2+}-release channel: activation by caffeine. *Am. J. Physiol.* 256: H328–H333.

Saito, A., M. Inui, M. Radermacher, J. Frank, and S. Fleischer. 1988. Ultrastructure of the calcium release channel of sarcoplasmic reticulum. *J. Cell Biol.* 107:211–219.

Stern, M. 1992. Theory of excitation-contraction coupling in cardiac muscle. *Biophys. J.* 63:497–517.

Stern, M., M. Capogrossi, and E. Lakatta. 1988. Spontaneous calcium release from the sarcoplasmic reticulum in myocardial cells: mechanisms and consequences. *Cell Calcium.* 9:247–256.

Takamatsu, T., and W. Wier. 1990. Calcium waves in mammalian heart: quantification of origin, magnitude, waveform, and velocity. *FASEB J.* 4:1519–1525.

Talo, A., M., Stern, H., Spurgeon, G., Isenberg, and E., Lakatta. 1990. Sustained subthreshold-for-twitch depolarization in rat single ventricular myocytes causes sustained calcium channel activition and sarcoplasmic reticulum calcium release. *J. Gen. Physiol.* 96:1085–1103.

Tang, Y. 1994. Theoretical Studies on Second Messenger Dynamics. University Microfilms Inc., Ann Arbor, Michigan. 263 pp.

Tang, Y., and H. Othmer. 1994. A G-protein-based model of adaptation in *Dictyostelium discoideum. Math. Biosci.* 120:25–76.

Wier, W. G., and L. Blatter. 1991. Ca^{2+}-oscillations and Ca^{2+}-waves in mammalian cardiac and vascular smooth muscle cells. *Cell Calcium.* 12:241–254.

Williams, D., L. Delbridge, S. Cody, P. Harris, and T. Morgan. 1992. Spontaneous and propagated calcium release in isolated cardiac myocytes viewed by confocal microscopy. *Am. J. Physiol.* 262:C731–C742.

Wong, A., A. Fabiato, and J. Bassingthwaigthe. 1992. Model of calcium-induced calcium release mechanism in cardiac cells. *Bull. Math. Biol.* 54:95–116.